Journal of Coordination Chemistry

ISSN: 0095-8972 (Print) 1029-0389 (Online) Journal homepage: http://www.tandfonline.com/loi/gcoo20

Four triarylantimony(V) carboxylates: syntheses, structural characterization and in vitro cytotoxicities

Honglin Geng, Min Hong, Yuanguang Yang, Dacheng Li, Xuetong Li, Fulin Liu & Meiju Niu

To cite this article: Honglin Geng, Min Hong, Yuanguang Yang, Dacheng Li, Xuetong Li, Fulin Liu & Meiju Niu (2015) Four triarylantimony(V) carboxylates: syntheses, structural characterization and in vitro cytotoxicities, Journal of Coordination Chemistry, 68:16, 2938-2952, DOI: 10.1080/00958972.2015.1060322

To link to this article: http://dx.doi.org/10.1080/00958972.2015.1060322

Accepted author version posted online: 22 Jun 2015.
Published online: 09 Jul 2015.

Journal of Coordination Chemistry, 2015
Vol. 68, No. 16, 2938–2952, http://dx.doi.org/10.1080/00958972.2015.1060322

Four triarylantimony(V) carboxylates: syntheses, structural characterization and *in vitro* cytotoxicities

HONGLIN GENG†, MIN HONG*†, YUANGUANG YANG†, DACHENG LI†, XUETONG LI‡, FULIN LIU‡ and MEIJU NIU†

†Shandong Provincial Key Laboratory of Chemical Energy Storage and Novel Cell Technology, School of Chemistry and Chemical Engineering, Liaocheng University, Liaocheng, China
‡The Second Middle School of Chiping County, Liaocheng, China

(*Received 18 December 2014; accepted 29 May 2015*)

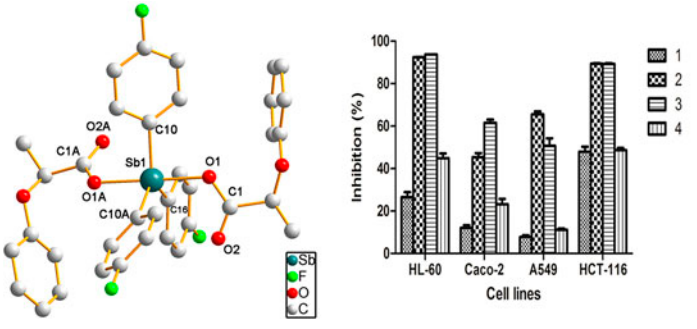

Four new organoantimony carboxylates, $(R–COO)_2SbR'_3$ [R–COOH = (±)-2-phenoxypropionic acid and R′ = phenyl (**1**), 4-fluorophenyl (**2**), 3-fluorophenyl (**3**), 3,4,5-trifluorophenyl (**4**)], were synthesized and structurally characterized by elemental analysis, ^1H, ^{13}C NMR, IR and X-ray single crystal diffraction. Structural analyses reveal that **1–3** show similar five-coordinate trigonal bipyramidal geometries, binding with three aryl groups and two deprotonated unidentate ligands. Unexpectedly, **4** exhibits pentagonal bipyramidal arrangement accompanied by two Sb–O (carbonyl) coordination bonds. *In vitro* cytotoxic activities of **1–4** have been determined by the MTT method against four cancer cell lines. Studies reveal that **1–4** have an activity similar to cisplatin on lung cancer cell line A549 and but also exhibit excellent cytotoxicity against cisplatin-insensitive colon cancer cell lines HCT-116, Caco-2 and human promyelocytic leukemia cell line HL-60. Additionally, the results showed that most of these triarylantimony(V) complexes exhibited enhanced cytotoxicity compared with the ligand and four triarylantimony dichloride precursors, which clearly implied a positive synergistic effect. Also interestingly, it was found that 3- or 4- mono-fluoro-substituted triphenylantimony, compounds **2** and **3**, exhibit higher *in vitro* cytotoxicities toward the four cancer cell lines than the tri-3,4,5-trifluoro-substituted and without-fluoro-substituted triphenylantimony complexes. The structure-activity relationship of the cytotoxicity of **1–4** is discussed.

Keywords: Organoantimony(V); (±)-2-Phenoxypropionic acid; Crystal structure; MTT; Cytotoxic activities

*Corresponding author. Email: hongmin@lcu.edu.cn

1. Introduction

The quest for alternative drugs to the well-known cisplatin and its derivatives, which are still used in more than 50% of the treatment regimes for patients suffering from cancer, is needed [1]. Despite their tremendous success, the use of Pt anticancer drugs is restricted by severe toxicity and by spontaneous or acquired resistance [2]. To overcome these limits, a number of other metal compounds have been investigated over the years. Organometallic compounds have a structural variety (ranging from linear to octahedral and even beyond) and far more diverse stereochemistry than organic compounds. By rational ligand design, organometallic compounds can provide control over key kinetic properties (such as hydrolysis rate of ligands). An increasing number of organoantimony(V) complexes have received attention not only for their fascinating structural diversities from discrete monomeric molecular species to associated structures and supramolecular compounds [3–7], but also for their biological activities [8–11].

Therapeutic values of antimony have been recognized for more than 100 years, and the major clinical use of antimony compounds is as a treatment for leishmaniasis [12, 13] and acute promyelocytic leukemia [14]. Because of the high cytotoxicity of antimony compounds against a broad spectrum of tumor cells, the potential anticancer properties of organoantimony(V) compounds have been investigated for two decades. In contrast to general expectations, evidence suggests that organoantimony(V) compounds exert their antiproliferative activities through mechanisms that are substantially different from those of platinum drugs. Yet, the molecular mechanisms and targets of antimony(V)-based antitumor metallodrugs remain largely uncharacterized.

It has been widely accepted that the ligands associated with the metal atom in complexes play an important role during their transport and assimilation at the membrane level and inside the cell. The cytotoxicity of organoantimony compounds depends on the coordination number and nature of groups bound to the central antimony atom [15]. Therefore, in order to replace the Pt-associated anticancer drugs with suitable alternatives, considerable attempts have been made to synthesize organoantimony(V) complexes, such as organoantimony carboxylates, organoantimony sulphonates and organoantimony oximes [16–21], and some of them have been reported to exhibit great antitumor activities. To investigate the influence of the number and electron-withdrawing ability of F atom on the cytotoxic activity of compounds, four different organoantimony(V) salts, that is tri-phenyl, tri-4-fluorophenyl, tri-3-fluorophenyl or tri-3,4,5-trifluorophenylantiomony dichlorides, were selected as reactants in our previous report [22]. Studies reveal that, in the case of the same structure (six-coordinate cyclic structure) and ligand [(±)-mandelic acid], the cytotoxicity against three cell lines [human lung carcinoma (A549), colon carcinoma (HCT-116) and colon adenocarcinoma (Caco-2)] tends to enhance with increase of the number of F atoms, that is, 3,4,5-3F-substituted > 4-F-substituted ≈ 3-F-substituted > without fluoro-substituted. To further investigate this effect, a chiral (±)-2-phenoxypropionic acid ligand was selected to react with the same four triarylantimony dichlorides. In the present study, four five- or pseudo-seven-coordinate organoantimony(V) compounds were obtained, which are different from the six-coordinate cyclic structures mentioned above, resulting from the absence of hydroxyl group in this ligand. The efficacy of four new compounds in suppressing the growth of a panel of human cancer cell lines was evaluated *in vitro*.

In addition, the carboxylate group can coordinate to metals in many ways, including as a unidentate ligand, chelating ligand, or bridging bidentate ligand [23]. Therefore, we are also interested in studying the structures of these pentavalent organoantimony complexes Ar_3Sb

$(O_2CR)_2$ and the influences of electronic and steric effects of aryl groups bound to antimony on the coordination geometry of the antimony center.

2. Experimental

2.1. *Materials and measurements*

Triphenylantimony dichloride and (±)−2-phenoxypropionic acid were commercially available and used without purification. The fluoro-substituted triarylantimony dichlorides were prepared according to the modified literature method [24]. Analytical grade solvents used in this work were dried before use. Elemental analyses were performed on a PE-2400-II elemental analyzer. IR spectra were recorded on a Nicolet-5700 spectrophotometer using KBr disks. ^{1}H and ^{13}C NMR spectra were recorded on a Varian Mercury Plus-400 NMR spectrometer. Chemical shifts were given in ppm relative to Me_4Si (^{1}H, ^{13}C) in $CDCl_3$ or DMSO solvent.

2.2. *Syntheses of 1–4*

2.2.1. $[PhO(Me)CHCO_2]_2Sb(C_6H_5)_3$ (1). The reaction was carried out under air with the use of standard Schlenk technique. 2-Phenoxypropionic acid (0.665 g, 4 mmol) and potassium hydroxide (0.224 g, 4 mmol) were added to methanol (80 mL) and heated under reflux with stirring for 0.5 h. After the addition of triphenylantimony dichloride (0.848 g, 2 mmol) to the reactor, the reaction mixture was refluxed for 8 h more. The reaction solution thus obtained was filtered and evaporated under vacuum to form a white solid, and then recrystallized from dichloromethane-petroleum ether (v/v 3 : 1) to give colorless single crystals of **1**. Yield: 74%, m.p.: 156–159 °C. Anal. Calcd for: $C_{36}H_{33}O_6Sb$: C, 63.27; H, 4.87%. Found: C, 63.31; H, 4.90%. IR (KBr, cm^{-1}): 1664 ν(C=O), 1375 ν(C–O), 433 ν(Sb–C), 461 ν(Sb–O). ^{1}H NMR (400 MHz, $CDCl_3$, ppm): 7.80–6.58 [m, 25H, Ph–Sb, Ph(O–CH)]; 4.46 (q, 2H, J = 6.8 Hz, –CH–); 1.32 (d, 6H, J = 6.8 Hz, CH_3–); ^{13}C NMR (100 MHz, $CDCl_3$, ppm): 175.55 (COO); 158.14; 136.72, 134.23, 131.41, 129.46, 129.42, 120.93, 115.03 (aryl group); 73.22 (–CH–); 18.56 (CH_3–).

2.2.2. $[PhO(Me)CHCO_2]_2Sb(4\text{-}FC_6H_4)_3$ (2). The procedure was the same as that of **1** and crystalline **2** was formed in dichloromethane-petroleum (v/v 3 : 1). Colorless block-shaped crystals of **2** were slowly formed at room temperature. Yield: 78%, m.p.: 162–164 °C. Anal. Calcd for: $C_{36}H_{30}F_3O_6Sb$: C, 58.63; H, 4.10%. Found: C, 58.66; H, 4.06%. IR (KBr, cm^{-1}): 1660 ν(C=O), 1371 ν(C–O), 433 ν(Sb–C), 466 ν(Sb–O). ^{1}H NMR (400 MHz, $CDCl_3$, ppm): 7.76–6.58 [m, 22H, C_6H_4–Sb, Ph(O–CH)]; 4.48 (q, 2H, J = 6.8 Hz, –CH–); 1.32 (d, 6H, J = 6.8 Hz, CH_3–); ^{13}C NMR (100 MHz, $CDCl_3$, ppm): 176.03 (COO); 163.51, 158.00, 136.36, 131.74, 129.44, 121.18, 116.73, 114.93 (aryl group); 73.06 (–CH–); 18.54 (CH_3–).

2.2.3. $[PhO(Me)CHCO_2]_2Sb(3\text{-}FC_6H_4)_3$ (3). Complex **3** was prepared in the same way as **1**. The colorless solid was then recrystallized from dichloromethane-petroleum (v/v 3 : 1).

Colorless block-shaped crystals of **3** were slowly formed at room temperature. Yield: 76%, m.p.: 159–163 °C. Anal. Calcd for: $C_{36}H_{30}F_3O_6Sb$: C, 58.63; H, 4.10%. Found: C, 58.64; H, 4.12%. IR (KBr, cm^{-1}): 1666 ν(C=O), 1373 ν(C–O), 441 ν(Sb–C), 477 ν(Sb–O). ^{1}H NMR (400 MHz, $CDCl_3$, ppm): 7.54–6.58 [m, 22H, C_6H_4–Sb, Ph(O–CH)]; 4.53 (q, 2H, J = 6.8 Hz, –CH–); 1.35 (d, 6H, J = 6.8 Hz, CH_3–); ^{13}C NMR (100 MHz, $CDCl_3$, ppm): 176.35 (COO); 164.05, 161.55, 157.86, 138.22, 131.01, 129.75, 129.50 121.24, 119.08, 114.86 (aryl group); 72.81 (–CH–); 18.52 (CH_3–).

2.2.4. $[PhO(Me)CHCO_2]_2Sb(3,4,5\text{-}F_3C_6H_2)_3$ (4). Complex **4** was prepared in the same way as **1**. The colorless solid was then recrystallized from dichloromethane-petroleum (v/v 3 : 1). Colorless block-shaped crystals of **4** were slowly formed at room temperature. Yield: 80%, m.p.: 179–181 °C. Anal. Calcd for: $C_{36}H_{24}F_9O_6Sb$: C, 51.15; H, 2.46%. Found: C, 51.13; H, 2.47%. IR (KBr, cm^{-1}): 1640 ν(C=O), 1367 ν(C–O), 439 ν(Sb–C), 482 ν(Sb–O). ^{1}H NMR (400 MHz, $CDCl_3$, ppm): 7.38–6.87 [m, 16H, C_6H_2–Sb, Ph(O–CH)]; 4.63 (q, 2H, J = 6.8 Hz, –CH–); 1.37 (d, 6H, J = 6.8 Hz, CH_3–); ^{13}C NMR (100 MHz, $CDCl_3$, ppm): 178.21 (COO); 157.44, 150.34, 141.24, 132.48, 129.54, 121.71, 118.44, 114.62 (aryl group); 72.11 (–CH–); 18.38 (CH_3–).

2.3. *X-ray crystallographic studies*

Diffraction data for the **1–4** were obtained on a Bruker Smart 1000 CCD diffractometer (graphite monochromated Mo Kα radiation, λ = 0.71073 Å). All data were corrected using SADABS and the final refinement was performed by full-matrix least-square methods with anisotropic thermal parameters for non-hydrogen atoms on F^2 using SHELX-97. The hydrogens were added theoretically, riding on the concerned atoms and refined with fixed thermal factors. Crystallographic data and experimental details of the structure determinations are listed in table 1.

2.4. *In vitro cytotoxicities*

2.4.1. Cell lines and culture conditions. The cell lines, human promyelocyticfina leukemic cell line (HL-60), human lung cancer cell line (A549) and human colon cell line (HCT-116, Caco-2) were used for screening. Cell lines were maintained in the logarithmic phase at 37 °C in a 5% carbon dioxide atmosphere using the following culture media containing 10% fetal bovine serum and 1% antibiotics (50 units mL^{-1} penicillin and 50 µg mL^{-1} streptomycin): (a) RPMI-1640 medium for HL-60 cells, (b) D-MEM (Dulbecco's Modified Eagle Medium) medium for A549 cell, (c) McCoy's 5A medium for HCT-116 cells, (d) I-MDM medium for Caco-2 cells.

2.4.2. Preparation of drug solutions. Stock solutions of the studied organoantimony compounds were prepared in DMSO (Sigma Aldrich) at concentrations of 10 mg mL^{-1} and diluted by cell culture medium to various working concentration. DMSO was used due to solubility problems. MTT, 3-(4,5-dimethylthiazol-2-yl)-2,5-diphenyl tetrazolium bromide was dissolved (5 mg mL^{-1}) in phosphate buffer saline pH 7.2 and filtered through Millipore filter, 0.22 mm, before use.

Table 1. Crystal data and structure refinement parameters for **1–4**.

Complex	**1**	**2**	**3**	**4**
Empirical formula	$C_{36}H_{33}O_6Sb$	$C_{36}H_{30}F_3O_6Sb$	$C_{36}H_{30}F_3O_6Sb$	$C_{36}H_{24}F_9O_6Sb$
Formula weight	683.37	737.35	737.35	845.30
Temperature (K)	298(2)	298(2)	293(2)	298(2)
Crystal system	Monoclinic	Monoclinic	Monoclinic	Orthorhombic
Space group	*C2/c*	*C2/c*	*C2/c*	Pnma
a (Å)	19.8929(18)	16.4596(17)	20.7781(19)	13.5960(12)
b (Å)	9.5080(10)	10.3241(7)	9.6908(8)	14.2959(13)
c (Å)	16.6801(17)	19.231(2)	16.2854(12)	17.3781(15)
α (°)	90	90	90	90
β (°)	90.2140(10)	99.1370(10)	93.651(7)	90
γ (°)	90	90	90	90
Volume (Å^3)	3154.9(5)	3226.5(5)	3272.5(5)	3377.7(5)
Z	4	4	4	4
Calculated density (g cm^{-3})	1.439	1.518	1.497	1.662
Absorption coefficient (mm^{-1})	0.919	0.918	0.905	0.913
F(0 0 0)	1392	1488	1488	0.913
Crystal size (mm)	0.44 × 0.36 × 0.12	0.50 × 0.48 × 0.45	0.42 × 0.39 × 0.31	0.40 × 0.32 × 0.25
θ range for data collection (°)	2.67–25.02	2.49–25.02	2.51–25.01	2.38–25.02
Reflections collected	7661	7808	9829	16,199
Independent reflections	2780	2835	2900	3107
R(int)	0.0334	0.0354	0.0745	0.0425
Max. and min. transmission	0.8977 and 0.6879	0.6829 and 0.6569	0.7668 and 0.7025	0.8039 and 0.7116
Data/restraints/parameters	2780/0/197	2835/0/211	2900/36/215	3107/6/252
Goodness-of-fit on F^2	1.035	1.099	1.054	1.155
Final *R* indices [$I > 2\sigma(I)$]	$R_1 = 0.0304$, $wR_2 = 0.0663$	$R_1 = 0.0344$, $wR_2 = 0.0826$	$R_1 = 0.0537$, $wR_2 = 0.1126$	$R_1 = 0.0393$, $wR_2 = 0.0895$
R indices (all data)	$R_1 = 0.0380$, $wR_2 = 0.0711$	$R_1 = 0.0406$, $wR_2 = 0.0872$	$R_1 = 0.0804$, $wR2 = 0.1260$	$R_1 = 0.0682$, $wR_2 = 0.1145$

2.4.3. Cytotoxicity assays. The colorimetric MTT assay was used to determine the cytotoxicity of **1–4**. All cells were seeded into a 96-well plate at cell densities of 1000–1500 cells/well, respectively, in 100 μL of growth medium and were incubated for 24 h. The medium was then removed and 200 μL of new growth medium containing various concentrations of the organoantimony(V) complexes was added. After 48 h, the medium was removed, 100 μL of a 0.5 mg mL^{-1} solution of MTT in medium was added, and the plate was incubated for an additional 4 h. The medium/MTT mixture was aspirated and 100 μL of DMSO were added to dissolve the purple formazan crystals. The plate was shaken for 10 min on a plate shaker to ensure complete dissolution. The absorbance of the plates was read at 490 nm. IC_{50} values were extrapolated from the resulting curves. The reported IC_{50} values are the averages from at least three independent experiments, each of which consisted of three replicates per concentration level.

3. Results and discussion

3.1. *Syntheses of organoantimony(V) compounds*

All the complexes are colorless crystalline solids. Complexes **1–4** were synthesized by reactions of triarylantimony dichlorides (denoted as **M**: $\mathbf{M_1}$–$\mathbf{M_4}$ hereafter) and the (±)-2-phe-

noxypropionic acid ligand in the presence of potassium hydroxide. All compounds are stable in air and soluble in chloroform, acetone, DMSO, mixture of water/DMSO. The synthetic procedures are shown in scheme 1.

3.2. *IR spectra*

IR spectra of **1–4** were recorded from 4000 to 400 cm^{-1}. The IR spectroscopic data provide further support for the molecular constitution of these compounds. By comparing the IR spectra of the complexes with the free (±)-2-phenoxypropionic acid, a remarkable difference is the complete disappearance of the stretching vibration of O–H (3254 cm^{-1}), indicating the deprotonation of hydroxyl group and formation of Sb–O bond [25]. The formation of Sb–O bond is further supported by the appearance of a weak to medium intensity band at 461–482 cm^{-1}, which is assigned to the Sb–O stretch [26]. In addition, the frequencies of Sb–C deformations appear between 433 and 439 cm^{-1}, consistent with the literature [27].

3.3. *NMR spectra*

In the ^{1}H NMR chemical shifts, the aromatic protons show a complicated multiplet between 6.58 and 7.80 ppm. All the protons in the compounds have been identified and the total number of protons calculated from the integration curve tallies with what is expected from the molecular formula. The ^{1}H NMR spectra of the ligand show a signal for the –COOH proton at 10.37 ppm which is absent in the complexes, indicating removal of the proton and formation of the Sb–O bond. This is consistent with the IR data. The ^{1}H and ^{13}C NMR spectra of **1–4** did not show significant changes in signal positions of the aryl groups as compared to those of the initial organoantimony chlorides.

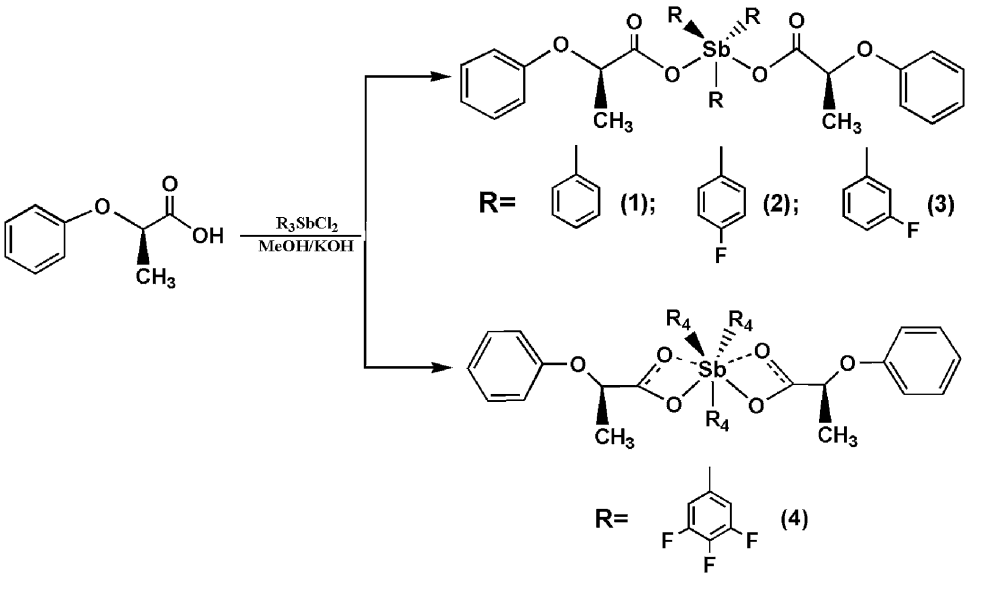

Scheme 1. The reaction procedures.

3.4. *Crystal structures*

3.4.1. Crystal structures of 1, 2 and 3. Complexes **1**, **2** and **3** have similar molecular structures, as illustrated in figures 1, 3 and 5. Selected bond lengths and angles of **1–3** are listed in table 2. For **1**, **2** and **3** the coordination environment of Sb(V) is a distorted trigonal bipyramid with three C of phenyl groups occupying the equatorial positions, and the axial positions of the trigonal bipyramid being occupied by two oxygens from the ligand. The sum of the angles subtended at the antimony in the equatorial plane is 360.01° for **1**, 360.02° for **2** and 360.0° for **3**. So for Sb(1), three phenyl groups occupy the equatorial positions, almost in the same plane. The angles of the axial O(1)–Sb(1)–O(1)#1 [175.20 (12)° for **1**, 178.23(13)° for **2**, 175.1(2)° for **3**] slightly deviate from the linear angle of 180°. Thus, the coordination geometry of the antimony center is best described as a distorted trigonal bipyramid. The Sb–O distances [between 2.088(5) and 2.124(2) Å] are typical bond lengths for carboxylate oxygen and triorganoantimony [27]. This indicate that there is very strong coordination interaction between the carbonyl oxygen and antimony. In **1**, **2** and **3** there also exist intermolecular hydrogen bonds, which are listed in table 3. As shown in figures 2, 4 and 6, the supramolecular structures of **1**, **2** and **3** are dominated by a 1-D infinite chain, which is involved in C–H···O (for **1**) and C–H···F (for **2** and **3**) hydrogen bonding. These hydrogen bonds contribute to the crystal stability and compactness.

3.4.2. Crystal structure of 4. The molecular structure of **4** is shown in figure 7 (see scheme 1 for line diagrams). Selected bond lengths and angles are listed in table 4. Carboxylates are versatile ligands which can be either unidentate or bidentate. The molecule

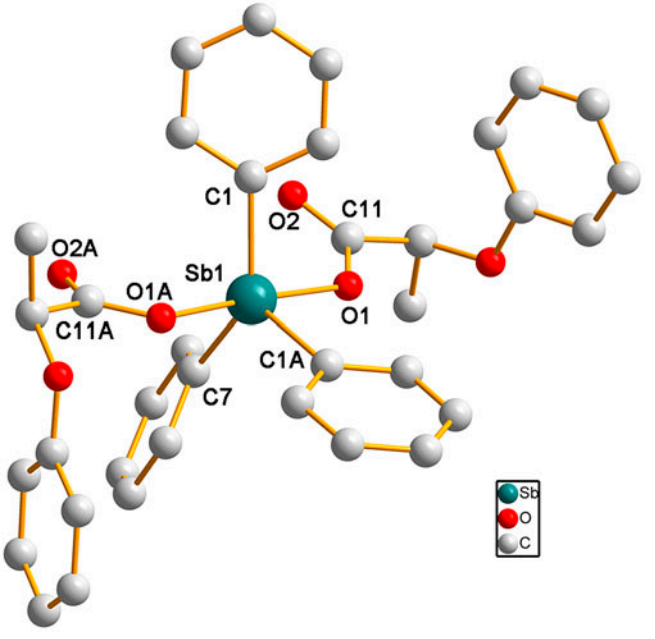

Figure 1. The molecular structure of **1**. All hydrogens are omitted for clarity.

Table 2. Selected bond lengths (Å) and angles (°) for **1**, **2** and **3**.

Complex **1**			
Sb(1)–O(1)	2.0975(19)	Sb(1)–O(1)#1	2.0975(19)
Sb(1)–C(1)	2.118(3)	Sb(1)–C(1)#1	2.118(3)
Sb(1)–C(7)	2.116(4)		
O(1)–Sb(1)–O(1)#1	175.20(12)	O(1)–Sb(1)–C(7)	87.60(6)
O(1)#1–Sb(1)–C(7)	87.60(6)	O(1)–Sb(1)–C(1)#1	89.91(10)
O(1)#1–Sb(1)–C(1)#1	91.94(10)	C(7)–Sb(1)–C(1)#1	112.65(9)
O(1)–Sb(1)–C(1)	91.94(10)	O(1)#1–Sb(1)–C(1)	89.91(10)
C(7)–Sb(1)–C(1)	112.65(9)	C(1)#1–Sb(1)–C(1)	134.71(18)
Complex **2**			
Sb(1)–O(1)	2.124(2)	Sb(1)–O(1)#1	2.124(2)
Sb(1)–C(10)	2.103(3)	Sb(1)–C(10)#1	2.103(3)
Sb(1)–C(16)	2.096(5)		
O(1)–Sb(1)–O(1)#1	178.23(13)	C(10)–Sb(1)–O(1)	92.95(11)
C(10)–Sb(1)–O(1)#1	86.12(10)	C(10)#1–Sb(1)–O(1)	86.12(10)
C(10)#1–Sb(1)–O(1)#1	92.95(11)	C(10)#1–Sb(1)–C(10)	117.13(18)
C(16)–Sb(1)–O(1)	90.88(6)	C(16)–Sb(1)–C(10)	121.43(9)
C(16)–Sb(1)–C(10)#1	121.43(9)	C(16)–Sb(1)–O(1)#1	90.88(6)
C(1)–O(1)–Sb(1)	118.1(2)		
Complex **3**			
Sb(1)–O(1)	2.090(4)	Sb(1)–O(1)#1	2.090(4)
Sb(1)–C(10)	2.104(6)	Sb(1)–C(10)#1	2.104(6)
Sb(1)–C(16)	2.113(8)		
O(1)–Sb(1)–O(1)#1	175.1(2)	O(1)–Sb(1)–C(10)	92.15(19)
O(1)#1–Sb(1)–C(10)	89.65(19)	O(1)–Sb(1)–C(10)#1	89.65(19)
O(1)#1–Sb(1)–C(10)#1	92.15(19)	O(1)–Sb(1)–C(16)	87.57(11)
O(1)#1–Sb(1)–C(16)	87.57(11)	C(10)–Sb(1)–C(10)#1	136.7(3)
C(10)–Sb(1)–C(16)	111.65(17)	C(10)#1–Sb(1)–C(16)	111.65(17)
C(1)–O(1)–Sb(1)	120.2(4)		

Notes: Symmetry transformations used to generate equivalent atoms: **1** #1 $-x, y, -z + 1/2$; **2** #1 $-x + 1, y, -z + 1/2$; **3** #1 $-x + 2, y, -z + 1/2$.

Table 3. Hydrogen bonding geometries for **1**–**4**.

D–H···A	d(D–H)	d(H···A)	d(D···A)	<(DHA)
Complex **1**				
C(4)–H(4)···O(2)#1	0.93	2.62	3.514(5)	160.7
Complex **2**				
C(9)–H(9)···F(2)#1	0.93	2.53	3.227(6)	132.5
Complex **3**				
C(18)–H(18)···F(1)#1	0.93	2.37	3.142(4)	140.8
Complex **4**				
C(19)–H(19)···F(5)	0.93	2.53	3.325(5)	144.3
C(15)–H(15)···F(3)	0.93	2.47	3.285(5)	145.8

Notes: Symmetry codes: (#1 for **1**) $x, y, -z + 1/2$; (#1 for **2**) $-x + 1, y, -z + 1/2$; (#1 for **3**) $-x + 2, y, -z + 1/2$.

consists of a monomer with a seven-coordinate antimony surrounded by four oxygens and three aryl groups. The coordination geometry of antimony is a distorted pentagonal bipyramid with four oxygens atoms [O(1), O(2), O(1)#1 and O(2)#1] from two asymmetrically chelating carboxylate groups and one carbon C(10) from one phenyl group occupying the equatorial positions, and two carbons [C(14) and C(20)] from phenyl groups occupying the axial positions. The sum of the angles subtended at the antimony in the equatorial plane is 360.0°, so Sb(1), C(10), O(1), O(2), O(1)#1 and O(2)#1 are in the same plane. The angle of

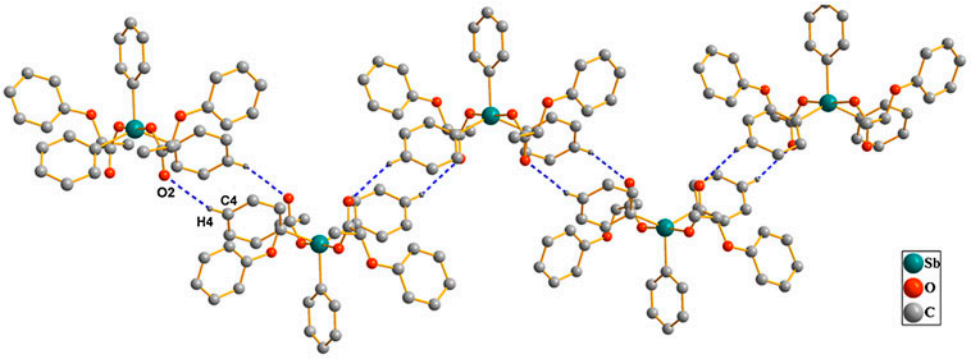

Figure 2. The 1-D chain structure of **1**, formed by intermolecular C–H···O hydrogen-bonding interactions. All hydrogens are omitted for clarity.

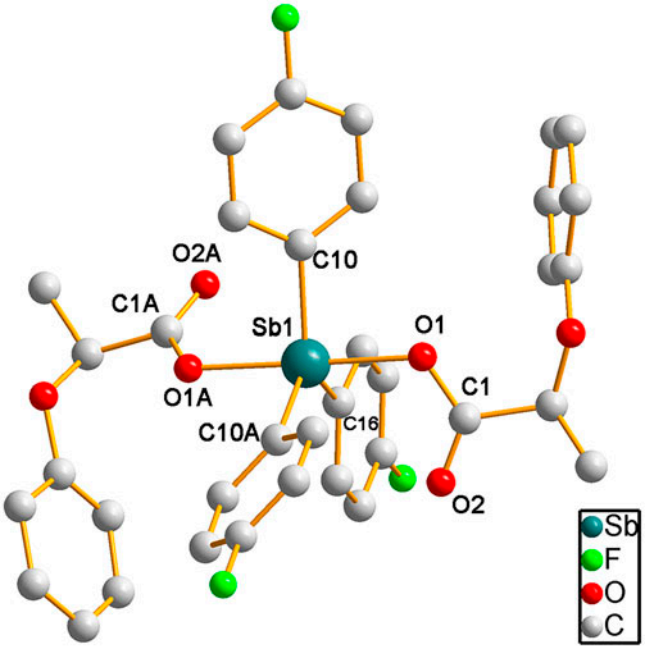

Figure 3. The molecular structure of **2**. All hydrogens are omitted for clarity.

the axial C(14)–Sb(1)–C(20) is 149.4(3)°, which deviates from the linear angle of 180°. The conformation of Sb(1) is considered to exhibit distorted pentagonal bipyramidal geometry.

In this compound, there are relatively strong bonding interactions between Sb(1) and the carbonyl oxygens of the carboxylates, Sb(1)–O(1) [or Sb(1)–O(1)#1, 2.141(3) Å)] (#1: x, $-y + 1/2$, z). However the intramolecular Sb(1)···O(2) distance of 2.621(3) Å is longer than the general Sb and O bond length (2.05–2.3 Å [23, 27]), but is still well within the sum of the van der Waals radii (3.60 Å) [28]. This indicates that there are coordination interactions

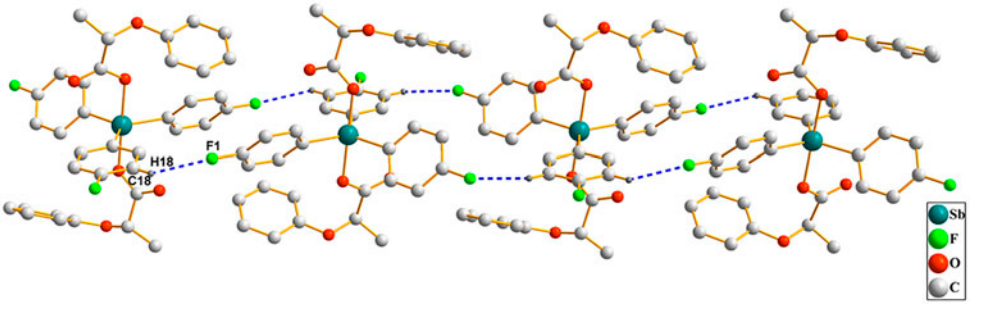

Figure 4. The 1-D chain structure of **2**, formed by intermolecular C–H···F hydrogen-bonding interactions. All hydrogens are omitted for clarity.

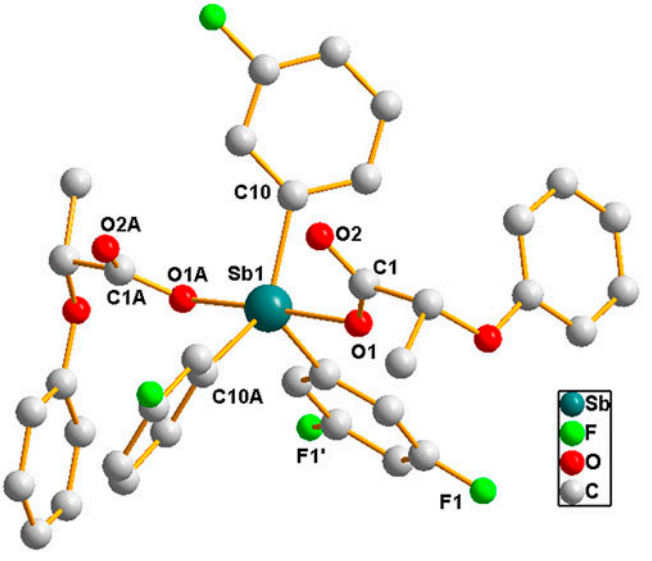

Figure 5. The molecular structure of **3**. All hydrogens are omitted for clarity.

between the carbonyl oxygens of the two asymmetrical carboxylate groups and antimony. Compared with the structures of **1–3**, the structural difference of **4** can be attributed to strong $-I$ effect of F of the aryl groups in the molecule. The $-I$ effect of three F atoms enhances the Lewis acidity of Sb and leads to the stronger Sb···O=C coordination [29]. As shown in figure 8, a 1-D infinite chain structure of **4** is formed by C–H···F hydrogen bonds. These hydrogen bonds contribute to the crystal stability and compactness (table 3).

3.5. *In vitro cytotoxicities*

By means of MTT assays [30, 31], the *in vitro* cytotoxicities of **1–4** along with their metal salts $\mathbf{M_1}$–$\mathbf{M_4}$, free **L** and the clinical antitumour agent cisplatin towards a panel of established human cancer cell lines, human lung carcinoma cell line (A549), human colon cell

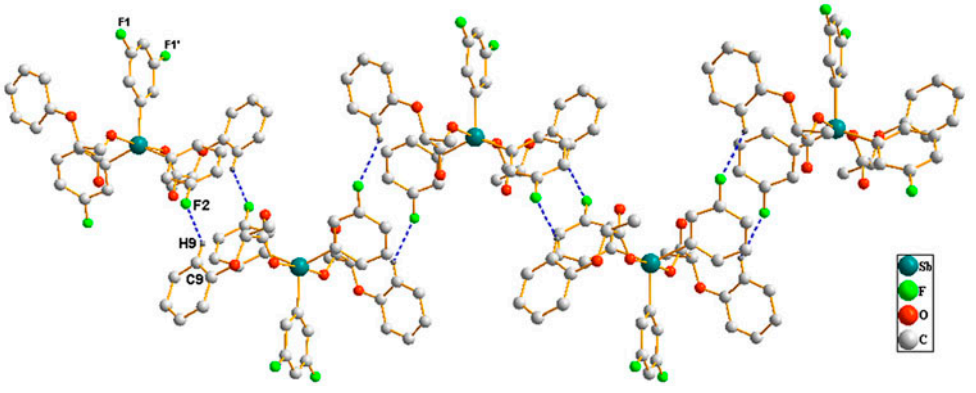

Figure 6. The 1-D chain structure of **3**, formed by intermolecular C–H···F hydrogen-bonding interactions. All hydrogens are omitted for clarity.

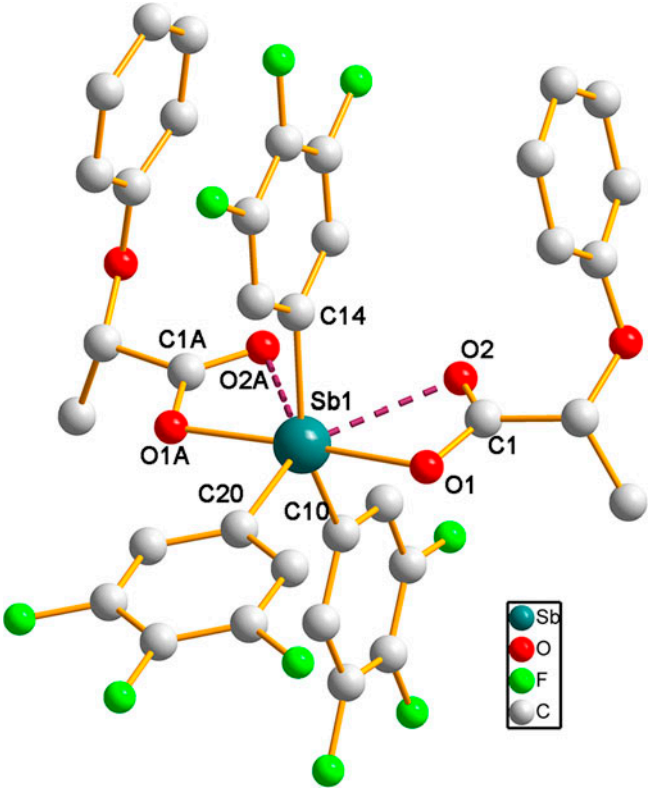

Figure 7. The molecular structure of **4**. All hydrogens are omitted for clarity.

line (HCT-116, Caco-2) and human leukemia cell line (HL-60), were measured. The antitumor activities *in vitro* are expressed as IC_{50}, the concentration of compound (in μg mL^{-1}) that inhibits a proliferation rate of the tumor cells by 50% as compared to control untreated

Table 4. Selected bond lengths (Å) and angles (°) for **4**.

Sb(1)–O(1)	2.141(3)	Sb(1)–O(1)#1	2.141(3)
Sb(1)–C(10)	2.134(3)	Sb(1)–C(14)	2.113(6)
Sb(1)–C(20)	2.124(7)	Sb(1)–O(2)	2.621(3)
Sb(1)–O(2)#1	2.621(3)		
C(14)–Sb(1)–O(1)	90.00(9)	C(20)–Sb(1)–O(1)	91.40(9)
C(10)–Sb(1)–O(1)	87.36(14)	C(14)–Sb(1)–O(1)#1	90.00(9)
C(20)–Sb(1)–O(1)#1	91.40(9)	C(10)–Sb(1)–O(1)#1	87.36(14)
C(1)–O(1)–Sb(1)	103.2(3)	O(1)–Sb(1)–O(1)#1	174.51(18)
C(14)–Sb(1)–C(20)	149.4(3)	C(14)–Sb(1)–C(10)	105.7(2)
C(20)–Sb(1)–C(10)	104.9(2)	C(14)–Sb(1)–O(2)	77.55(17)
C(20)–Sb(1)–O(2)	78.87(18)	C(10)–Sb(1)–O(2)	140.82(14)
O(1)–Sb(1)–O(2)	53.46(12)	O(1)#1–Sb(1)–O(2)	131.81(12)
C(14)–Sb(1)–O(2)#1	77.55(17)	C(20)–Sb(1)–O(2)#1	78.87(18)
C(10)–Sb(1)–O(2)#1	140.82(14)	O(1)–Sb(1)–O(2)#1	131.81(12)
O(1)#1–Sb(1)–O(2)#1	53.46(12)	O(2)–Sb(1)–O(2)#1	78.36(16)
C(1)–O(2)–Sb(1)	82.4(3)		

Note: Symmetry transformations used to generate equivalent atoms: #1 x, $-y + 1/2$, z.

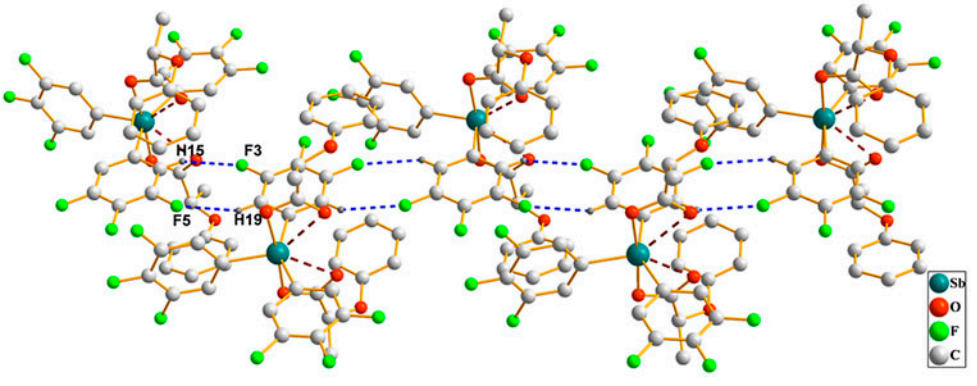

Figure 8. The 1-D chain structure of **1**, formed by intermolecular C–H···F hydrogen-bonding interactions. All hydrogens are omitted for clarity.

cells. IC_{50} values for **1–4**, four triarylantimony dichlorides, the ligand and cisplatin obtained after 48 h of drug treatment in the MTT test are listed in table 5 and the inhibition effects of **1**, **2**, **3** and **4** on the four cells lines at a concentration of 10 μg mL^{-1} are listed in figure 9. Based on these data, the possible structure-activity relationships are:

(1) The four triarylantimony dichlorides exhibit a relatively weak activity although the HL-60 cell proliferation can be inhibited to some extent. The ligand is non-active to the determined cancer cells. Most of these triarylantimony complexes have *in vitro* cytotoxicity not only against cisplatin-sensitive lung cancer cell line A549 but also against cisplatin-insensitive colon cancer cell lines HCT-116, Caco-2 and human promyelocytic leukemia cell line HL-60. Additionally, these four triarylantimony complexes exhibited enhanced cytotoxicity compared with (±)-2-phenoxypropionic acid ligand and the triarylantimony dichloride precursors, which clearly implied a positive synergistic effect against all four cancer cell lines. Among these four compounds, **2** and **3** exhibit excellent activity against all the cancer cells.

Table 5. IC_{50} (μg mL^{-1}) of all compounds against four human tumor cell lines.

	HL-60	Caco-2	A549	HCT-116
1	16.1 ± 1.2	27.7 ± 1.5	>60	15.5 ± 1.2
2	2.5 ± 0.4	12.4 ± 1.1	9.3 ± 1.0	3.9 ± 0.6
3	1.4 ± 0.2	10.9 ± 1.0	13.52 ± 1.1	3.6 ± 0.6
4	12.3 ± 1.1	21.8 ± 1.3	32.9 ± 1.5	11.3 ± 1.1
$\mathbf{M_1}$	7.159 ± 0.9	40.5 ± 3.2	36.6 ± 2.9	45.0 ± 3.2
$\mathbf{M_2}$	7.848 ± 0.9	26.6 ± 2.7	25.0 ± 2.4	24.0 ± 2.1
$\mathbf{M_3}$	6.947 ± 0.8	29.8 ± 2.3	26.3 ± 2.6	20.0 ± 2.0
$\mathbf{M_4}$	6.156 ± 0.8	26.5 ± 2.0	25.6 ± 2.0	12.2 ± 1.4
L	>100	>100	>100	>100
Cisplatin	>60	>60	3.3 ± 0.2	>60

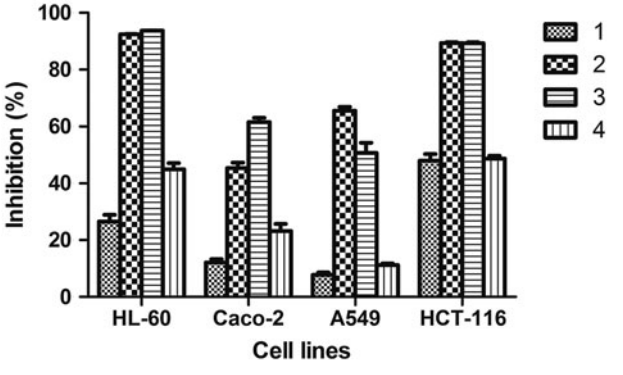

Figure 9. Inhibition (%) of **1–4** (dose level of 10 μg mL^{-1}) against human tumor cells.

(2) Each organoantimony compound exhibited different inhibition for different tumor cells. With **3**, for example, about 10-fold improvement of the antitumor potency in HL-60 cells compared to A549 cells, 3-fold improvement in HCT-116 cells than Caco-2 cells.
(3) **1**, **2** and **3** have similar coordination geometry. Fluoro-substituted **2** and **3** exhibit higher activity compared with **1**, indicating the fluoro-substituent has a positive effect on cytotoxic activities. This is consistent with the result we reported previously [22] and many other reports [14, 32]. However, tri-3,4,5-trifluoro-substituted **4** exhibits lower activity than 3- or 4- mono-fluoro-substituted triphenylantimony **2** and **3**, which is contrary to the result previously [22]. This may be because of their different coordination geometry. Though the activity mechanism of these compounds is unclear, further studies are required for establishing clear relationships with the activity.

4. Conclusion

Four new organoantimony(V) derivatives were synthesized by reaction of 2-phenoxypropionic acid with four different triarylantimony dichlorides, which have also been evaluated for their *in vitro* anticancer activities. Structural analyses show that **1–3** have distorted trigonal bipyramidal geometries, while **4** exhibits pentagonal bipyramidal arrangement

coordinated by the bidentate chelating ligand. Preliminary *in vitro* anticancer studies against a variety of cancer cell lines reveal that mono-fluoro-substituted **2** and **3** show better antitumor activity on four cancer cell lines than **1** and **4**. **2** and **3** are highly active against HL-60 and HCT-116 tumor cell lines, making them promising anticancer agents in cisplatin-insensitive cell lines, whereas **1** shows the lowest IC_{50} on A549 cells. Our results suggest that in the case of the same structure, 3- or 4-F-substituted triarylantimony(V) compounds show higher cytotoxicity than triphenylantimony(V) compound, consistent with our previous report [22]. However, due to the structural difference, 3,4,5-3F-substituted compound display lower cytotoxicity than 3- or 4-F-substituted triarylantimony(V) compounds. These studies are useful in the initial cytotoxicity screening, with the intention of selecting the best performing compound for subsequent studies involving a much larger pool of human cancers and *in vivo* experiments.

Supplementary material

CCDC 871822 (for **1**), 980782 (for **2**), 980783 (for **3**) and 980784 (for **4**) contain the supplementary crystallographic data for this paper. These data can be obtained free of charge via http://www.ccdc.cam.ac.uk/conts/retrieving.html, or from the Cambridge Crystallographic Data Center, 12 Union Road, Cambridge CB2 1EZ, UK; Fax: (+44) 1223-336-033; or Email: deposit@ccdc.cam.ac.uk.

Acknowledgements

We acknowledge the National Natural Foundation of China (21105042), the Science Foundation of China Postdoctor (2014M560572) and the Natural Science Foundation of Shandong Province (ZR2013BM017) for financial support. And this work was supported by Shandong "Tai–Shan Scholar Research Fund".

Disclosure statement

No potential conflict of interest was reported by the authors.

References

[1] (a) P.C. Bruijnincx, P.J. Sadler. *Curr. Opin. Chem. Biol.*, **12**, 197 (2008); (b) L. Kell. *Nat. Rev. Cancer*, **7**, 573 (2007); (c) M. Markman. *Drug Saf.*, **2**, 597 (2003).
[2] D. Wang, S.J. Lippard. *Nat. Rev. Drug Discov.*, **4**, 307 (2005).
[3] A. Gupta, R.K. Sharma, R. Bohra, V.K. Jain, J.E. Drake, M.B. Hursthouse, M.E. Light. *Polyhedron*, **21**, 2387 (2002).
[4] H.D. Yin, J. Zhai. *Inorg. Chim. Acta*, **362**, 339 (2009).
[5] L. Quan, H.D. Yin, J.C. Cui, M. Hong. *J. Organomet. Chem.*, **694**, 3683 (2009).
[6] H.D. Yin, J. Zhai, Y.Y. Sun. *Polyhedron*, **27**, 663 (2008).
[7] V.K. Jam, R. Bohra, R.C. Mehrotra. *Struct. Bonding*, **52**, 147 (1982).
[8] R.C. Liu, Y.Q. Ma, L. Yu, J.S. Li, J.R. Cui, R.Q. Wang. *Appl. Organomet. Chem.*, **17**, 662 (2003).
[9] E.R.T. Tiekink. *Crit. Rev. Oncol./Hematol.*, **42**, 217 (2002).

[10] A. Bara, C. Socaciu, C. Silvestru, I. Haiduc. *Anticancer Res.*, **11**, 1651 (1991).
[11] F. Wang, H.D. Yin, C.H. Yue, S. Cheng, M. Hong. *J. Organomet. Chem.*, **738**, 35 (2013).
[12] J.D. Berman. *Rev. Infect. Dis.*, **10**, 560 (1988).
[13] M.B. Lee, H.M. Gilbert. *Infect. Med.*, **16**, 37 (1999).
[14] P. Sharma, D. Perez, A. Cabrera, N. Rosas, J.L. Arias. *Acta Pharmacol. Sin.*, **29**, 881 (2008).
[15] F. Asghar, A. Badshah, A. Shah, M.K. Rauf, M.I. Ali, M.N. Tahir, E. Nosheen, Z. Rehman, R. Qureshi. *J. Organomet. Chem.*, **717**, 1 (2012).
[16] L. Quan, H.D. Yin, J.C. Cui, M. Hong, D.Q. Wang. *J. Organomet. Chem.*, **694**, 3708 (2009).
[17] S. Bredeau, E. Ortega, G. Delmas, P. Richard, R. Fröhlich, B. Donnadieu, G. Kehr, N. Pirio, G. Erker, P. Meunier. *Organometallics*, **28**, 181 (2009).
[18] K.H. Chan, W.K. Leong, K.H.G. Mak. *Organometallics*, **25**, 250 (2006).
[19] W.W. Qin, S.J. Yasuike, N. Kakusawa, Y. Sugawara, M. Kawahata, K. Yamaguchi, J. Kurita. *J. Oragnomet. Chem.*, **693**, 109 (2008).
[20] M. Hong, H.D. Yin, W.K. Li, X.Y. You. *Inorg. Chem. Commun.*, **14**, 1616 (2011).
[21] L.G. de Oliveira, M.M. Silva, F.C.S. de Paula, E.C. Pereira-Maia, C.L. Donnici, C.A. de Simone, F. Frézard, E.N. da Silva Júnior, C. Demicheli. *Molecules*, **16**, 10314 (2011).
[22] J. Jiang, H.D. Yin, F.L. Wang, Z. Han, F. Wang, S. Cheng, M. Hong. *Dalton Trans.*, **42**, 8563 (2013).
[23] Y.Q. Ma, J.S. Li, Z.A. Xuan, R.C. Liu. *J. Organomet. Chem.*, **620**, 235 (2001).
[24] R.F. De Ketelaere, F.T. Delbeke, G.P. Van Der Kelen. *J. Organomet. Chem.*, **30**, 365 (1971).
[25] H.D. Yin, C.H. Yue, M. Hong, J.C. Cui, Q.K. Wu, X.Y. Zhang. *Eur. J. Med. Chem.*, **58**, 533 (2012).
[26] S.S. Garje, V.K. Jain. *Main Group Met. Chem.*, **18**, 387 (1995).
[27] L. Yu, Y.Q. Ma, R.C. Liu, G.C. Wang, J.S. Li, G.H. Du, J.J. Hu. *Polyhedron*, **23**, 823 (2004).
[28] A. Bondi. *J. Phys. Chem.*, **68**, 441 (1964).
[29] M.N. Gibbons, D.B. Sowerby. *J. Organomet. Chem.*, **555**, 271 (1998).
[30] (a) F. Denizot, R. Lang. *J. Immunol. Methods*, **89**, 271 (1986); (b) P. Skehan, R. Storeng, D. Scudiero, A. Monks, J. McMahon, D. Vistica, J.T. Warren, H. Bokesch, S. Kenney, M.R. Boyd. *J. Natl. Cancer Inst.*, **82**, 1107 (1990).
[31] P. Price, T. McMillan. *Cancer Res.*, **50**, 1392 (1990).
[32] G.C. Wang, Y.N. Lu, J. Xiao, L. Yu, H.B. Song, J.S. Li. *J. Organomet. Chem.*, **690**, 151 (2005).